PREDICTION OF PAYLOAD RANDOM VIBRATION LOADS

Y. T. Chung
Principal Engineer, Structural Dynamics
Space Station Division
McDonnell Douglas Aerospace - West
5301 Bolsa Avenue
Huntington Beach, California 92647

B. L. Foist
Senior Engineer. Structural Dynamics
Space Station Division
McDonnell Douglas Aerospace-West
5301 Bolsa Avenue
Huntington Beach, California 92647

ABSTRACT

This paper examines the prediction of National Space Transportation System (NSTS) payload random vibration loads. In the past. spacecraft random vibration loads were approximated as equivalent static loads using Miles equation. A technique for predicting random vibration loads using the finite element method is described for NSTS payloads. The random vibration loads predicted by this finite element approach will be compared with those computed by Miles equation and the sensitivity of the random loads due to the pressure field forcing functions will be examined. The benefits of this approach are the use of similar dynamics and vibroacoustics finite element models and the ease of combining transient and vibroacoustic loads.

NOMENCLATURE

A	Panel Area Excited by Random Vibration
f_n	Natural Frequency (Hz)
$G(\omega)$	Input Power Spectra Density
$H_{ja}(\omega)$	Frequency Response Function
$P(\omega)$	Input Forcing Function
Q	Dynamic Amplification Factor or $1/2\zeta$
$\dot{R}_j(\tau)$	Autocorrelation Function
rms	Root Mean Square
$S_j(\omega)$	Power Spectra Density at Location j
T	Time
$\overline{u_{g's}}$	Acceleration rms Response (G_{rms})
$u_t(t)$	Output Response
W	Weight (lb)
γ	Narrowband Spatial Correlation Function
κ	Wave Number
λ	Wave Length
ω	Frequency (rad/sec)
ζ	Viscous Damping
σ	Standard Deviation
	Complex Conjugate

1 INTRODUCTION

Spacecraft structures are usually exposed to three major dynamic environments that generate structural loads. High frequency acoustic loads are induced by excitations resulting from engine generated noise during static firing and liftoff, and from in-flight fluctuating pressures during ascent and reentry. Random vibration loads are acoustically and mechanically induced by engine generated excitations. Low frequency structural loads, which include transient loads, are generated by launch vehicle liftoff and landing events [1]. Acoustic and random vibration loads have bean treated as secondary loads in the past and were approximated as equivalent static loads using Miles equation [2]. Miles equation assumes that the random response is dominated by the acceleration spectral density at a specific resonant frequency and the coupling between the input excitations and the structural resonant frequencies is insignificant. These assumptions introduce conservatism in the response of a component responding to acoustic dynamic pressure. A recent study [3] also indicates that the vibroacoustic load components occurring simultaneously with the transient load components, especially the mechanically transmitted random loads, can be a significant part of the total structural loads of a payload.

Two methods have been used in predicting the random vibration loads, the finite element method (FEM) and statistical energy analysis method (SEA). The FEM is generally used to compute loads for low frequencies and SEA is used for the high frequency region. However, the FEM is a more preferable approach for computing the mechanically transmitted loads due to the FEM capabilities in describing the structural members and the low modal density per third octave band in the low frequency range for a system. Test loads for structural verification are based upon the combination of random vibration and transient loads. The major drawback of the FEM approach in predicting the random vibration loads is the modeling and implementation of the forcing functions describing the pressure fields.

The NSTS cargo bay acoustic pressure field is a function of the external acoustics, noise reduction by transmission loss and absorption of the cargo bay walls. volume of the unfilled cargo bay and acoustic treatments of the payload. The internal acoustics excite payload acoustic receivers with large area-to-weight ratios producing random vibration loads. For NSTS payloads the maximum random response occurs during launch at approximately four seconds after Solid Rocket Booster (SRB) ignition [4]. The mechanically transmitted random vibrations less than 35 Hz are assumed to be included in the transient launch excitation. The acoustically induced random environment is assumed to behave as reverberant sound field. In a reverberant sound field all waves have been incident and reflected many times from the wall boundaries over a random variation of angles. At high frequencies a reverberant field tends to behave like a diffused sound field with uncorrelated pressure sources. At low frequencies a reverberant field is spatially correlated and can excite all structural resonances in the low frequency range [5].

2 ACOUSTICS AND RANDOM VIBRATION

Random vibration is a phenomena that is described by its statistical properties. Random responses as a function of time are unknown while the probability that a random response being within a certain range is known. The methods for predicting the random loads assume stationary ergodic processes [6]. For a stationary normal random process with zero mean, the statistical peak of a function is three times the standard deviation or root mean square (rms) value [7]. As shown in Figure 1, the rms value squared is the area under the power spectral density function. At a 99.7 percent confidence level, all responses for a normal random process are between a 3σ response interval of the response mean. A 3σ response in a random analysis is comparable to a maximum and minimum value in a transient analysis.

MSC/NASTRAN treats random analysis as a data reduction procedure that is applied to the frequency response analysis. The theory is described in Reference 8 and some concepts are defined below.

The mean value, $\overline{u_j(t)}$, is given by

$$\overline{u_j(t)} = \lim_{T\to\infty}\frac{1}{T}\int_0^T u_j(t)dt \tag{1}$$

The autocorrelation function is defined by

$$R_j(\tau) = \lim_{T\to\infty}\frac{1}{T}\int_0^T u_j(t)u_j(t-\tau)dt \tag{2}$$

The power spectral density over positive frequencies is defined by

$$S_j(\omega) = \lim_{T\to\infty}\frac{2}{T}\left|\int_0^T u_t(t)e^{-i\omega t}dt\right|^2 \tag{3}$$

or

$$S_j(\omega) = \lim_{T\to\infty}\frac{2}{T}u_j(\omega)u_j^*(\omega) \tag{4}$$

Using Fourier transforms the autocorrelation and power spectral density functions can be expressed as Fourier transform pairs.

$$R_j(\tau) = \frac{1}{2\pi}\int_0^\infty S_j(\omega)\cos(\omega\tau)d\omega \tag{5}$$

The mean square value of the response is found from

$$\overline{u_j(t)^2} = \frac{1}{2\pi}\int_0^\infty S_j(\omega)d\omega \tag{6}$$

The square of the rms value of the response is evaluated as the area under the power spectral density function. For a ergodic normal random process with zero mean. $\overline{u_j(t)} = 0$, the standard deviation and rms value are equivalent.

$$\sigma = \sqrt{\overline{u_j(t)^2} - \left(\overline{u_j(t)}\right)^2} = \sqrt{\overline{u_j(t)^2} - (0)} \tag{7}$$

and

$$rms = \sqrt{\overline{u_j(t)^2}} \tag{8}$$

The equation of motion of a system under dynamic loading can be expressed as

$$[M]\ddot{x}(t) + [D]\dot{x}(t) + [K]x(t) = \{P(\omega)\}e^{i\omega t} \tag{9}$$

Let the solution be of the form $x(t) = u(\omega)e^{i\omega t}$.

$$-\{[M]\omega^2 + i[D]\omega + [K]\}u(\omega) = P(o) \tag{10}$$

The frequency response function. $H_{ja}(\omega)$, relates the output $u_j(\omega)$ to the input $P_a(\omega)$.

$$u_j(\omega) = H_{ja}(\omega)P_a(\omega) \tag{11}$$

The power spectral density of the response, $S_j(\omega)$, is related to the PSD of the source, S,(w), by

$$S_j(\omega) = |H_{ja}(\omega)|^2 S_a(\omega) \tag{12}$$

where the input spectra is

$$S_a(\omega) = \lim_{T\to\infty}\frac{2}{T}P_a(\omega)P_a^*(\omega) \tag{13}$$

If sources are statistically independent, the total response is equal to the sum of the PSD of the responses due to the individual sources as shown in equation (14).

$$S_j(\omega) = \sum_a \left|H_{ja}(\omega)\right|^2 S_a(\omega) \quad (14)$$

If the sources are statistically correlated, the degree of correlation can be expressed by a cross spectral density, $S_{ab}(\omega)$, and the power spectral density of the response may be evaluated from

$$S_j(\omega) = \sum_a \sum_b H_{ja}(\omega) H^*_{jb}(\omega) S_{ab}(\omega) \quad (15)$$

where $H_{jb}^*(\omega)$ is the complex conjugate of $H_{jb}(\omega)$.

A shortcoming of MSC/NASTRAN is complex frequency dependent description of the excitation load [5]. Frequency response solutions are calculated for a single frequency or frequency band. where the excitation is constant within the band. The fundamental frequencies of the system should be included in the set of analysis points to adequately predict peak response.

3 CORRELATION OF EXCITATIONS

Component response to acoustics is a function of the frequencies and mode shapes of the component, the acoustic pressure spectrum, the spatial correlation of the pressure spectrum over the component and the damping the component. Goyna [5] discusses the formulation of a spatial correlation function as a function of pressure spectra density, phase and narrowband spatial decay. The spatial decay rate characterizes the distance and frequency over which the pressure field is correlated. For a diffused pressure field, the cross spectra density reduces to the following [9]

$$S_{ab}(\xi, \eta, \omega) = S_{ab}(\omega) \frac{\sin(\kappa r)}{(\kappa r)} \quad (16)$$

$$S_{ab}(\xi, \eta, \omega) = S_{ab}(\omega)\gamma \quad (17)$$

where $\sin(\kappa r)/(\kappa r)$ denotes the narrowband spatial correlation, γ, and

$$\kappa = \frac{2\pi}{\lambda} \quad (18)$$

$$\lambda = \frac{V}{f} \quad (19)$$

$$r = \sqrt{\left(\xi^2 + \eta^2\right)} \quad (20)$$

The wavelength. λ, is a function of velocity, V, and frequency, f, for the acoustic source. The radial distance between two points on a component. r, is expressed in terms of normal coordinates ξ and η.

The narrowband spatial correlation function, γ, is plotted in Figure 2 for standard atmospheric conditions where the speed of sound is 1116.4 ft/sec. At low frequencies and small separation distances the spatial correlation function tends to a value of one and fully correlated inputs. At high frequencies and large separation distances spatial correlation effects decay a rate of $1/\kappa r$ and the input field simulates an uncorrelated input field. At the intermediate values of frequency and separation distances the spatial correlation effects are significant.

Bounding the spatial correlation function is recommended to limit the amount of the excitation data for random vibration loads analyses using the FEM approach. For a panel the sound pressure wavelength corresponding the fundamental panel mode is found by setting $\sin(\kappa r)/(\kappa r)$ equal to zero. If the pressure field wavelengths are greater than the dimensions of the panel, there is no need for surface integration of the spatial correlation function. For separation distances at a given frequency where $1/\kappa r$ is less than 0.1, the spatial correlation function becomes negligible and the excitations can be assumed to be uncorrelated.

4 FINITE ELEMENT APPROACH

With the FEM approach the acoustic environment is applied directly to the finite element model. The power spectral densities (dB) of the loading conditions are converted into pressure loads (psi) and applied to significant acoustic receivers. The profile of the pressure field excitation power spectral density is defined within the frequency range of interest.

NSTS flight data is available for estimating the orbiter cargo bay internal acoustic environment. The acoustic levels in an empty cargo that are defined in Reference 10 represent the minimum levels to which components must be certified. A 3 dB fill factor adjustment for large diameter payloads increases the pressure field in Reference 10 to the levels shown in Table 1. The acoustic levels during orbit, entry and landing are significantly below the ascent levels and are assumed negligible. The acoustic environment is converted from sound pressure levels in decibels to a pressure field PSD, $S_p(\omega)$, in terms of psi^2/Hz. The reference sound pressure is 2.9×10^{-6} psi.

In MSC/NASTRAN the acoustic pressure field in Table 1 is represented as pressure loads and discrete forces which are applied to acoustic receivers of the finite element model. Application of the acoustic pressure loads to a large finite element model can be a tedious task. By applying acoustic pressure loads to a subset of the entire system, the amount of input data can be reduced while not compromising the results. Acoustic receptors are those quadrilateral, triangular and beam elements which represent a significant exposed area and are responsive to acoustic pressure loads. On the International Space Station Alpha (ISSA) acoustic receptors are typically a panel with an area-to-weight ratio of greater than 10 in^2/lb. Figure 3 illustrates the acoustic receptors on ISSA segment S3/S4 including the Solar Alpha Rotary Joint (SARJ), Utility Carriers, Mobile Transporter Radiator, Avionics Panels, Thermal Control Subsystem (TCS) Radiator Panels, Photo Voltaic (PV) Array Containment Boxes, Beta Gimbal Mast Canister and Integrated Equipment Assembly. A free field pressure level of 141 dB Overall SPL. (OASPL). is applied to surfaces without structural interference. A 3 dB increase in the free field pressure level is applied to the elements which have structural interference or "wall effects" with other acoustic receivers.

Table 1 NSTS Cargo Bay Acoustic Environment

1/3 Octave Band Center Frequency (Hz)	Sound Pressure Level (dB)	Pressure Power Spectra Density (psi^2/Hz)
20.0	121.0	2.286E-06
25.0	123.0	2.899E-06
31.5	125.0	3.646E-06
40.0	127.0	4.551E-06
50.0	128.5	5.142E-06
63.0	130.0	5.765E-06
80.0	131.0	5.715E-06
100.0	131.5	5.130E-06
125.0	132.0	4.605E-06
160.0	132.0	3.598E-06
200.0	131.5	2.565E-06
250.0	130.0	1.453E-06
315.0	129.0	9.158E-07
400.0	128.0	5.729E-07
500.0	126.0	2.892E-07
630.0	124.5	1.625E-07
800.0	123.0	9.058E-08
1000.0	120.5	4.075E-08
1250.0	119.0	2.308E-08
1600.0	117.0	1.138E-08
2000.0	115.0	5.742E-09
2500.0	113.0	2.899E-09
OASPL	141.0	

For random vibration loads on ISSA cargo elements the excitation frequency range of interest is 20 to 200 Hz. A vibroacoustic development test is performed on an acoustic simulation of the a partial Space Station Freedom (SSF) Segment S2 as shown in Figure 4. Accelerometer and strain gage data were examined and some results are presented in Figure 5. The accumulated rms strain data begins to levels off at 120 Hz and remains relatively constant above 200 Hz [11]. The upper frequency represents a conservative estimate of the frequency beyond which stresses and strains in structural elements due to random vibration is negligible [12].

The damping profile of a random loads analysis for NSTS payloads is recommended by David Hamilton of NASANSC [13]. The modal damping schedule is given in Table 2 and is expressed as a percent of critical damping.

Table 2 NSTS Payload Modal Structural Damping for Random Loads Analysis

Frequency (Hz)	Modal Damping (ζ)
0.0	0.01
10.0	0.01
10.0	0.02
35.0	0.02
75.0	0.03
130.0	0.04
200.0	0.05

In MSC/NASTRAN power spectral density factor is defined on a RANDPS card and having the form

$$S_{ab}(\xi,\eta,\omega) = S_{ab}(\omega)\frac{\sin(\kappa r)}{(\kappa r)} = G(\omega)(X + iY) \quad (21)$$

For a reverberant sound field Y is assumed to be zero. With X equal to one the spatial correlation effects of the cross spectra density are input as a function of frequency on the TABRND1 card.

5 SENSITIVITY OF EXCITATION CORRELATION

The sensitivity of the random loads due to the degree of correlation between acoustic receiver components is examined. Numerical analyses are performed on the panels shown in Figures 6 and 7. Panel 1 is an aluminum plate with a uniform thickness of 0.5 inch. The panel is cantilevered along the bottom edge with a first natural frequency of 3.39 Hz. The second example is a simply supported plate made of aluminum with a constant thickness of 0.5 inch. Panel 2 has a first natural frequency of 11.18 Hz.

The random vibration analysis is executed from 0 to 250 Hz at a frequency resolution of 1 .O Hz. Both examples have a pressure field auto spectrum of 1.0 x 10^{-6} psi^2/Hz and modal damping of 1% over the frequency range. Acoustic excitations are applied to the quadrilateral plate elements within the zones shown in Figures 6 and 7. The zones are the equivalent to an acoustic receiver. The pressure field within each zone is assumed to be fully correlated. The sensitivity of the random vibration response to the cross spectra density is shown in Figures 8 through 11. The cross spectra density, $S_{ab}(\omega)$, is varied by setting the narrowband spatial correlation function. γ, equal to zero, one and $\sin(\kappa r)/(\kappa r)$. For γ equal to zero the excitations are uncorrelated and when γ equals one the excitations are fully correlated.

Figures 8 and 9 shows acceleration rms response as a function of grid location. Bending moment rms response is plotted in Figures 10 and 11. The maximum rms acceleration for panel 1 is 0.71 G_{rms} at grid 15 with partially correlated excitations. For panel 2 the maximum rms bending moment My for elements 1 and 2 is produced by the partially correlated excitations. This demonstrates that the responses due to the correlated and uncorrelated excitations are not bounds to the rms response versus excitation correlation envelope.

6 PREDICTION OF RANDOM VIBRATION LOADS

Historically, Miles equation has been used to calculate component response loads due to random vibration excitation. Miles equation assumes a single degree freedom system that is excited by white noise. In a practical sense the panel fundamental mode shape is assumed to be the same shape as the deflected shape for a uniform pressure, and the spatial correlation of the pressure field over the panel is uniform [1]. Given these assumptions the rms response is given by

$$\overline{u_{g's}} = \sqrt{\frac{\pi}{2} Q f_n S_{g's}} \tag{22}$$

where $u_{g's}$ and $S_{g's}$ are in G_{rms} and G_{rms}^2/Hz, respectively. The acceleration PSD, $S_{g's}$, in g^2/Hz can be evaluated from the pressure PSD, S_p, in psi^2/Hz as follows

$$S_{g's} = S_p(\omega)\left(\frac{A}{W}\right)^2 \tag{23}$$

where A and W are the panel area and weight of the component.

A random vibration response analysis is performed on the segment S3/S4. MSC/NASTRAN modal frequency response solution sequence is used to generate structural member loads and grid point accelerations. The first modal frequency of the segment is 6.93 Hz. The analysis is executed from 0 to 150 Hz with a frequency resolution of 1.0 Hz. The acoustic pressure loads are applied to acoustic receivers listed in Section 4. For this comparison the acoustic excitations are assumed to be fully correlated. The rms component loadfactor as computed by MSC/NASTRAN and Miles formula are compared in Table 3. The component loadfactor is defined as the acceleration at the component center of gravity. For the NSTS components studied, the finite element results for random vibration rms acceleration are less than those predicted by Miles equation.

Table 3 Random Loads Predicted by Miles Equation and Finite Element Model

Item	f_n (Hz)	Q	S_g (g^2/Hz)	Miles (G_{rms})	FEM (G_{rms})
MT Radiator	26.06	25	6.2×10^{-4}	0.79	0.18
UTC (+Y)	28.82	25	6.0×10^{-3}	2.61	1.90
UTC (-Y)	28.82	25	6.0×10^{-3}	2.61	1.97
TCS Radiator	24.65	25	1.2×10^{-2}	3.57	1.08

7 CONCLUSIONS

A technique for predicting random vibration loads using the finite element method is demonstrated for NSTS payloads. The random vibration loads predicted by the finite element approach are compared with those computed by Miles equation. For the NSTS payloads investigated, the finite element results for random vibration rms acceleration are less than those predicted by Miles equation. The sensitivity of the random loads due to the pressure field forcing functions is examined. The output responses due to correlated and uncorrelated excitations do not envelope the rms responses due to excitations with spatial correlation. Studies are currently being conducted to examine to significance of the spatial correlation on random loads prediction.

8 ACKNOWLEDGMENTS

The authors gratefully acknowledge the assistance of co-workers Robert Abercrombie, Kenneth Leung and Leland Smith.

9 REFERENCES

[1] '"Design and Verification Guidelines for Vibroacoustic and Transient Environments," NASA TM-86538, March 1986.

[2] Miles, J. W., "On Structural Fatigue Under Random Loading," Journal of Aerospace Science, Vol.21, No. 11, pp.753.762, 1954.

[3] Kern, D., Salama, M., and Smith, K., "Combined Loads Methodologies for Vibroacoustic and Transient Environments." 61st Shock and Vibration Symposium, Pasadena, CA, October 1990.

[4] Bonin, M. C.,"Liftoff Random Vibration Reduction Factors for Space Shuttle Payloads," Space Shuttle Payload/Cargo Integration Structures Technical Interchange Meeting, Downey, CA, May 19-20, 1992.

[5] Gloyna, F. L.,"Vibroacoustic Response Using the Finite Element Method and Statistical Energy Analysis," 59th Shock and Vibration Symposium, Albuquerque, NM, October 1988.

[6] MSC/NASTRAN Handbook for Dynamic Analysis, MSC/NASTRAN Version 63, The MacNeal-Schwendler Corporation, Los Angeles, CA, 1983.

[7] Thomson, W. T., Theory of Vibration with Applications, Prentice-Hall, Inc., Englewood Cliffs, N. J., pp.400-435, 1981.

[8] Crandall, S. H., and Mark, W. D., Random Vibration in Mechanical Systems, Academic Press, 1963.

[9] Cockburn, J. A.,and Jolly, A. C., "Structural-Acoustic Response of an Aircraft Fuselage Exited by Random Pressure Fields," AFFDL-TR-68-2, 1968.

[10] "Shuttle Orbiter/Cargo Standard Interfaces,' NASA ICD-2-19001, December 17, 1993.

[11] "Launch/On-Orbit Acoustic, Shock, Vibration. and Microgravity Analysis Report," MDA MDC93H0342, Contract No. NAS9-18200, Huntington Beach, CA, pp.108-130, March 1993.

[12] "Environet Loads and Lows Frequency Dynamics," AIAA Shuttle Environment and Operations II Conference, Houston, TX, November 1985.

[13] Hamilton. D. A.. informal memorandum between NASA/JSC and MDA, January 22.1992.

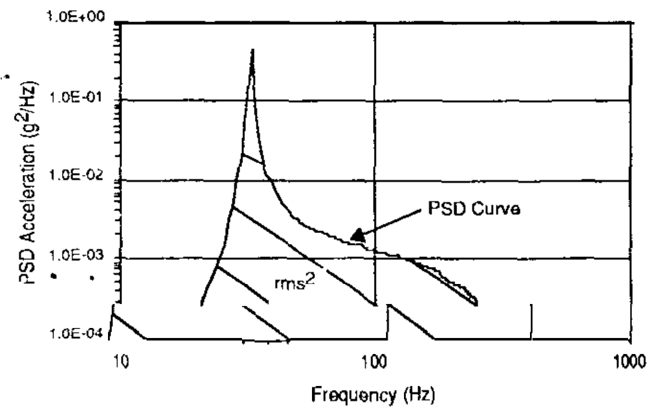

Figure 1 PSD and rms Relationship for Ergodic Processes

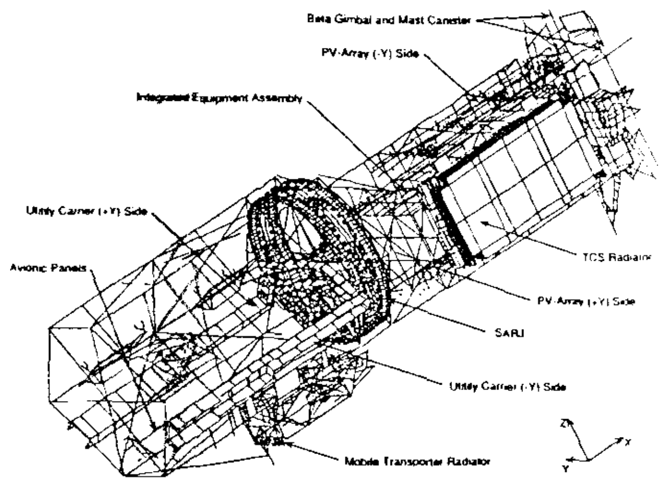

Figure 3 Segment S3/S4 Finite Element Model

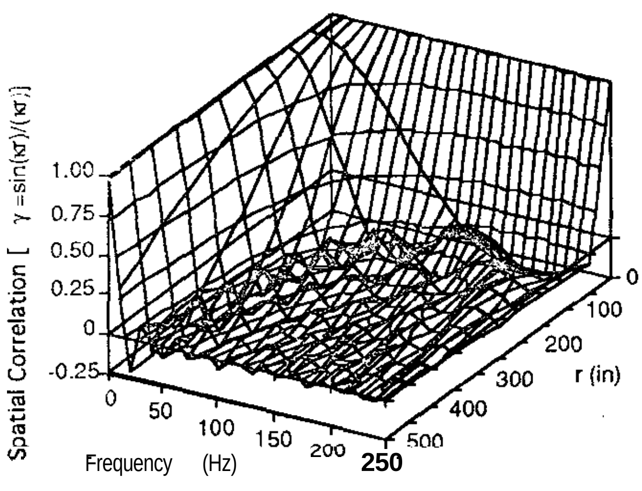

Figure 2 Narrowband Spatial Correlation Function, γ

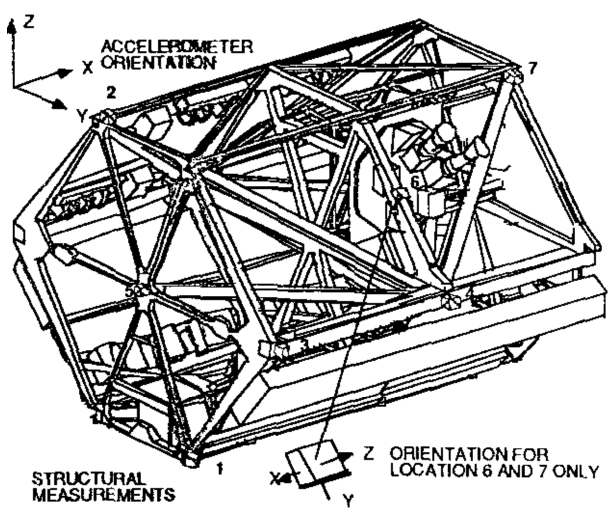

Figure 4 Partial Segment S2 Vibroacoustic Test Article

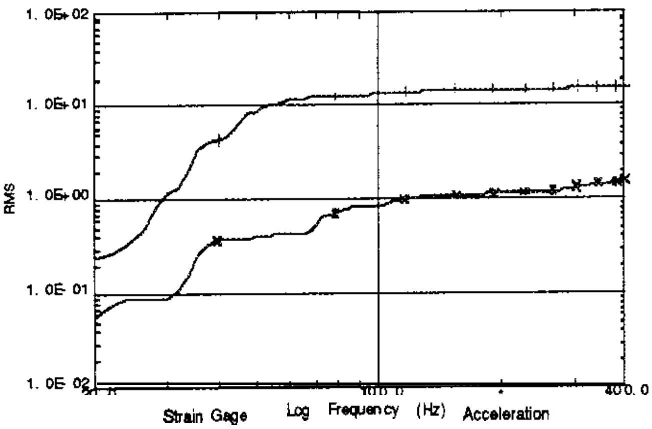

Figure 5 S2 Vibroacoustics Development Test Results

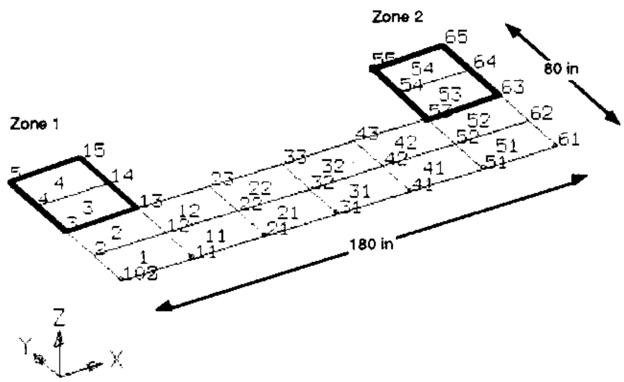

Figure 6 Panel 1 Finite Element Model

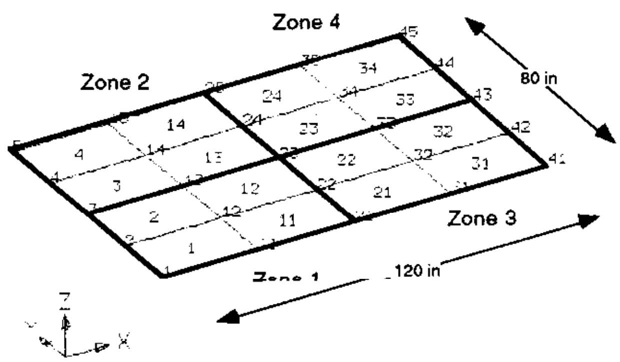

Figure 7 Panel 2 Finite Element Model

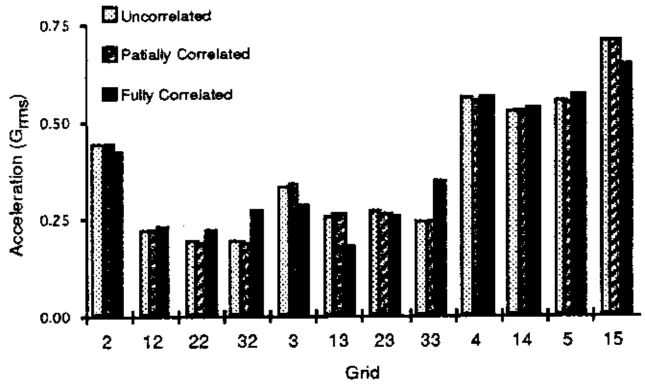

Figure 6 Panel 1 rms Accelerations

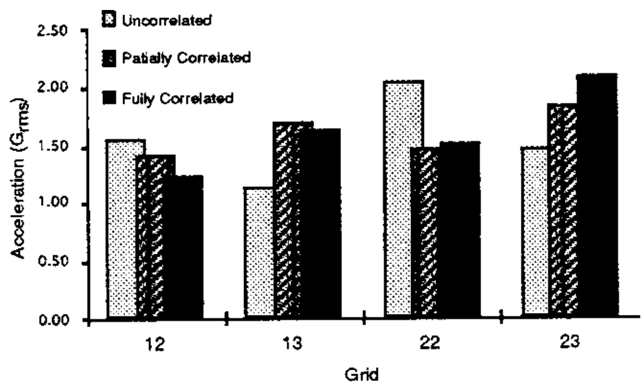

Figure 9 Panel 2 rms Accelerations

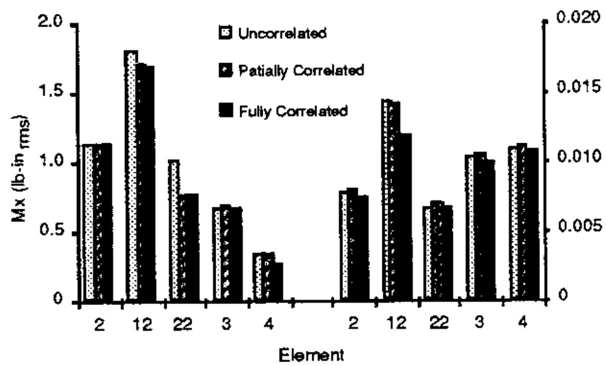

Figure 10 Panel 1 rms Bending Moments

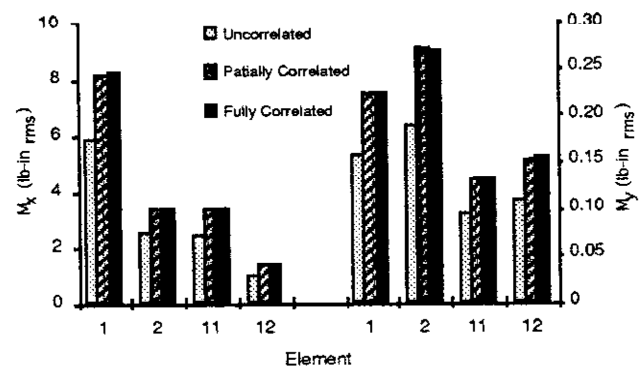

Figure 11 Panel 2 rms Bending Moments